Open-Source vs. Commercial Photogrammetry: Comparing Accuracy and Efficiency of OpenDroneMap and Agisoft Metashape

Adam Kostrzewa[1], Anna Płatek-Żak[1], Przemysław Banat[1], Łukasz Wilk[1]

[1]Warsaw University of Technology, Faculty of Geodesy and Cartography, Plac Politechniki 1, 00-661 Warsaw, Poland
(adam.kostrzewa.dokt, anna.platek, przemyslaw.banat.dokt, lukasz.wilk)@pw.edu.pl

Commission I

Keywords: UAV, photogrammetry, open-source software, OpenDronMap, Agisoft Metashape, low-cost technology

Abstract

The rapid advancement of drones and autonomous platforms has significantly enhanced the capabilities of aerial data acquisition. Drones, equipped with cameras, are now widely used in fields such as surveying, mapping, agriculture, or infrastructure inspections. The effectiveness of UAV (Unmanned Aerial Vehicle) platforms depends on factors such as data acquisition, software selection, and processing parameters, all of which influence the resulting products like orthomosaics and digital elevation models (DEMs). Both commercial and open-source software can process UAV data, each with its strengths and weaknesses. Commercial software typically offers higher accuracy but comes at a high cost, while open-source solutions provide a free alternative, though they are less intuitive for some users. OpenDroneMap (ODM), open-source software, offers similar functionalities to popular commercial options, enabling the generation of point clouds, DEMs, and mesh models using advanced algorithms like Multi-View Stereo (MVS) and Poisson surface reconstruction. On the other hand, Agisoft Metashape, a commercial software, is known for its user-friendly interface and comprehensive capabilities, making it popular for aerial imagery applications. In this paper, a comparison between ODM and Agisoft Metashape was conducted, focusing on their algorithms and processing performance. The results emphasize differences in camera calibration accuracy and data orientation. The study examined results from datasets acquired under various conditions. The findings revealed that ODM produces comparable results to Agisoft Metashape, the choice between the two depends on user requirements and specific project needs.

1. Introduction

UAVs equipped with RGB or multispectral cameras are widely used in fields like agriculture (e.g., Jełowicki et al., 2020), forestry (e.g., Näsi et al., 2018), or archaeology (e.g., Ostrowski et al., 2024). UAV equipment's affordability and broad availability have contributed to the growing number of users employing this technology for measurement purposes.

To obtain high-quality geospatial data from UAV imagery, it is necessary to process the images using specialized software that offers functions like camera calibration, orthophoto generation, and the creation of dense point clouds. Among the most popular commercial UAV image processing tools on the market are PIX4D Mapper and Agisoft Metashape (e.g., Pell et al., 2022). However, the high cost of commercial software often limits accessibility, especially for individual users. In recent years, open-source solutions have gained popularity in the photogrammetric community. A notable example in UAV image processing is OpenDroneMap (OpenDroneMap Authors, 2020).

Choosing the right software for UAV image processing is often a key factor affecting the quality of final outputs and the efficiency and cost-effectiveness of the processing workflow. This article compares two UAV image-processing software packages: the commercial Agisoft Metashape (version 2.1.3) and the open-source solution OpenDroneMap (ODM, version 3.5.0).

The study compares the workflow structure, algorithm implementation, and processing performance in both programs. We evaluate the processing pipelines with a primary focus on camera calibration and data orientation across different terrain types and processing scenarios.

1.1 Technical Overview: OpenDroneMap and Agisoft Metashape

ODM is a free and open-source software package designed for command line use, compatible with Linux, macOS, and Windows operating systems (OpenDroneMap Authors, 2020). It enables the UAV imagery processing into point clouds, digital elevation models (DEMs), textured surface models, and orthophotos (Patel et al., 2020). Since version 0.9.9, ODM has supported the multispectral imagery (MSI) processing. The software does not require a GPU to operate, but disk space and RAM affect image processing capacity. The official recommendation is to use 128 GB of RAM to process approximately 2,500 images (OpenDroneMap Authors, 2020). The other part of ODM is WebODM and offers a web-based interface and API, complete with tools for data visualization, storage, and analysis (OpenDroneMap Authors, 2020). Both software use the same core processing engine (Bgair et al., 2023).

ODM relies on several open-source libraries, including e. g., OpenSfM, OpenMVS, GDAL or PoissonRecon. OpenSfM handles feature extraction and matching and generates a sparse point cloud based on tie points. ODM then uses Multi-View Stereo (MVS) for 3D model reconstruction (OpenDroneMap Authors, 2020), a widely used technique for generating depth maps from multiple views (Shen, 2013). ODM also supports the filtering and classification of point clouds using the Simple Morphological Filter (SMRF) algorithm, enabling the generation of a Digital Terrain Model (DTM) from the point cloud.

In contrast, Agisoft Metashape is a commercial software. Its algorithms are based on computer vision techniques. Key advantages of Metashape include its intuitive user interface, extensive export capabilities, and support for automated processing via Python scripting. Its comprehensive functionality

https://doi.org/10.5194/isprs-archives-XLVIII-1-W4-2025-65-2025 |

for RGB and MSI data workflows has led to widespread adoption across the aerial imagery field.

The image processing workflow in both programs is similar and begins with importing image files and reading metadata from EXIF (Exchangeable Image File Format) tags about camera parameters and geolocation data. Both ODM and Metashape can estimate interior camera parameters and compute lens distortion coefficients during the photo alignment and 3D reconstruction. In ODM, the OpenSfM library handles feature extraction, matching, and sparse point cloud generation based on tie points. Metashape Align Photos algorithm uses the Structure from Motion technique and Bundle Adjustment procedure (Triggs et al., 1999; Agisoft LLC, 2025).

Both ODM and Metashape support calibration for various sensor types, including frame cameras, fisheye cameras, spherical cameras, and cylindrical cameras. Metashape offers full control over interior parameters and distortion coefficients. ODM uses predefined calibration parameter sets depending on the selected camera model, such as perspective, brown, fisheye, fisheye_opencv, spherical, equirectangular, and dual. Both programs also allow importing camera calibration parameters from external sources, such as laboratory calibration files. Metashape processes images at full (original - high) resolution or at reduced levels (lowest, low, medium). The highest level uses the original image resolution with enhanced feature filtering. ODM's ultra level similarly processes images at their native resolution during the feature-quality step, but each subsequent stage uses downscaled image pyramids—similar to Metashape—where the resolution is halved to accelerate processing and reduce the number of detected features. Metashape provides an advanced tools for analyzing camera calibration, including Radial, Decentering, Corrections, and Residual plots, as well as the Covariance matrix with correlation values for interior orientation parameters. ODM offers only a basic Residual Norm plot.

In the context of MSI image processing, ODM supports radiometric calibration to a limited extent. Radiometric calibration is essential for deriving reflectance values from images instead of digital number (raw pixel values). ODM supports "camera" and "camera+sun" calibration. Mode "camera" executes the calibration based only on sensor attributes such as black level, vignetting, gain gradients, or exposure compensation—if they are available in the EXIF tags. The "camera+sun" mode applies corrections that include all camera-based adjustments and additionally compensates for the sun irradiance as recorded by the downwelling light sensor in image metadata. Neither method allows the use of calibration panels. Omitting to use the calibration panel and relying only on the sun sensor may yield inconsistent and unreliable results (da Silva et al., 2024), requiring pre-processing outside of ODM.

Agisoft Metashape allows radiometric calibration using calibration panels, sun sensor or both. Using panels and sun sensor data is a common and recommended practice. In the case of using only panels, the software computes calibration coefficients for each photo based on values measured on masked photos of calibration panels and file containing calibration values for specific panel in a set range of wavelengths, while combined calibration (panels + sun sensor) also requires downwelling sun sensor metadata obtained from EXIF files. (Agisoft LLC, 2025)

2. Related works

There are already several studies comparing different UAV image processing software. Burdziakowski (2017) evaluated one of the first versions of ODM (version 0.3). Vacca (2020) compared three open-source software: ODM, VisualSfM, and Regard3D for the development of close-range images, where the final result was a point cloud generated based on the images. Mora-Felix et al. (2024) compared ODM with Metashape and Pix4D for DEM accuracy. Pell et. al. (2022) performed a comparison of WebODM (version 2.6.4) with Metashape, Correlator3D and Pix4Dmapper. Battle (2018) compared ODM with MicMac, E-photo, Mapillary and BundlerTools. Bgair et al. (2023) comprehensively described ODM (version 3.0) efficiency when working on different working platforms with different technical parameters (laptop, PC, virtual machine). Many authors compared the quality of the generated products in open-source software, e.g., ODM, and commercial software, e.g., Metashape (e. g. Vacca, 2020, Kloc et al., 2021, Nikolakopoulos & Koukouvelas, 2017, Silva et al., 2022).

Drone-mounted cameras are typically non-metric cameras (Przybilla et al., 2020). When using such images, the software should provide a complete workflow, from reliable calibration to accurate product generation. Camera calibration has a high impact on the quality and accuracy of the final products.

Both Metashape and ODM offer effective camera calibration and image orientation. Calibrating the camera and determining image orientation parameters is crucial to obtain accurate and reliable photogrammetric products (Garcia et al., 2020). Calibration is necessary to model systematic errors caused by lens distortion. Non-metric cameras, especially low-budget ones, are often characterised by instability and unknown interior orientation parameters (Garcia et al., 2020). There are various methods for camera calibration, including self-calibration, which is carried out as part of the measurement process. This is made possible by taking a greater number of images and using specialised software (Fryskowska-Skibniewska et al., 2016).

Image orientation is a procedure to determine the external orientation parameters of a set of images (Garcia et al, 2020). Traditional photogrammetric software has often been optimized to work with nadir images (Ostrowski & Bakuła, 2016). Oblique images characterized by different viewing angles and varying scale are challenging for traditional algorithms and software (Rupnik et al., 2013).

The accuracy of calibration and orientation of images is a subject of interest for researchers. Metashape is often used as a standard for comparing and testing other photogrammetric software (Vacca, 2019) due to its high and comparable accuracy (Garcia et al, 2020). Based on the work of Vacca (2019), Agisoft Metashape/PhotoScan software generally provides higher accuracy and reliability in a photogrammetric process (e.g., camera self-calibration) compared to ODM, although accuracy always depends on many factors, including input data quality and scene characteristics.

Many authors have compared ODM with other programmes. Often, however, these studies used older versions or did not specify a version. Software is constantly evolving to meet users' needs. Comparing open source and commercial software is therefore an ongoing research problem. This article uses the latest version of ODM and UAV imagery, making the proposed experiment a current research issue.

Regarding MSI data processing, Vivar-Vivar et al. (2022) used ODM for mixed forest monitoring based on multispectral indices. They did not mention the process or method of radiometric calibration, making it difficult to assess the reliability of the results. Nevertheless, ODM's ability to process images of a higher number of bands was demonstrated. Vong et al. 2021 emphasized availability and customizability of ODM in contrast to commercial solutions as they proposed an open-source based workflow on creating MSI and thermal 2D and 3D photogrammetric products. The paper did not mention ODM's radiometric calibration methods. ODM also has the functionality to compute alignment matrices of multi-lens sensors that correct

https://doi.org/10.5194/isprs-archives-XLVIII-1-W4-2025-65-2025

displacements between bands due to the camera design (OpenDroneMap repository, 2022).

3. Materials: Study area and datasets

This study aimed to compare the quality of camera orientation and self-calibration in two software environments: the open-source ODM and the commercial Metashape. The analysis used several multi-variant datasets, including nadir and oblique RGB imagery, with and without the use of ground control points (GCPs), as well as MSI data. The test scenarios are summarized in Table 1. The research data were divided into several processing scenarios. Scenarios 1a and 1b involved image processing at different resolution levels to evaluate its impact on the results. Scenarios 2a and 2b focused on processing with the use of GCPs, while scenario 3 addressed the processing of MSI imagery. Further details on the processing scenarios are provided in Methods.

RGB and MSI imagery from the DJI Mavic 3 Multispectral drone was acquired over the test site in Józefosław (JOZE), but only RGB data from JOZE we process. At the second test site in Herby, flights were performed using a DJI Phantom 4 RTK, capturing both nadir and oblique RGB images. This site was also equipped with signalized reference markers measured during a GNSS RTK survey conducted using a Leica VIVA GS15 receiver, providing reliable ground-truth data for the analysis. Figure 1 presents the distribution of measured points, including both GCPs and Check Points (ChPs), used to assess the accuracy of camera orientation and self-calibration. In the Herby oblique dataset, a total of 34 terrain points were used—5 GCPs and 29 ChPs. In the Herby nadir dataset, 64 points were distributed, including 7 GCPs and 57 ChPs. Additionally, a dataset of nadir MSI images was acquired over the Gołuchów site using a DJI Matrice 300 RTK equipped with the MicaSense RedEdge-MX Dual camera.

The flight plans at the JOZE and Gołuchów test sites followed a regular grid pattern, whereas the missions in Herby (nadir and oblique) and Gołuchów were designed as linear (corridor) flights. Figures 2–6 illustrate each test site along with its respective image acquisition layouts and flight trajectories.

Figure 1. Distribution of GCPs (green) and ChPs (red). Top: Herby (nadir), bottom: Herby (oblique)

The MicaSense RedEdge-MX Dual is a high-resolution MSI imaging system that captures data in ten narrow spectral bands, spanning key regions from coastal blue (444 nm) to near-infrared (842 nm). Its dual-sensor configuration enables detailed vegetation and environmental analysis by combining visible, red-edge, and NIR wavelengths.

All three UAV platforms used in this study (Phantom, Mavic, and Matrice) are equipped with dual-frequency GNSS receivers, providing the basis for direct georeferencing of aerial imagery using RTK or PPK positioning techniques. According to manufacturer specifications, the expected positioning accuracy is 1.5 cm + 1 ppm (vertical) and 1.0 cm + 1 ppm (horizontal), expressed as root mean square error (RMS) (DJI 2025a, DJI 2025b, DJI 2025c).

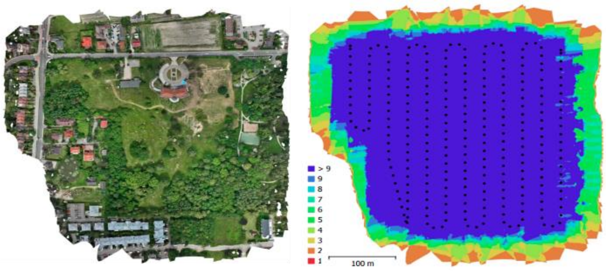

Figure 2. Overview of the image datasets acquired in JOZE, used in scenarios 1a (RGB)

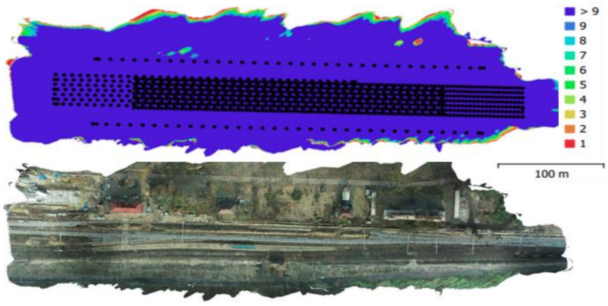

Figure 3. Overview of the oblique RGB image datasets acquired in Herby (scenarios 1b and 2b)

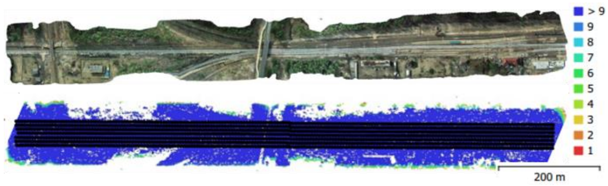

Figure 4. Overview of the nadir RGB image datasets acquired in Herby (scenario 2a)

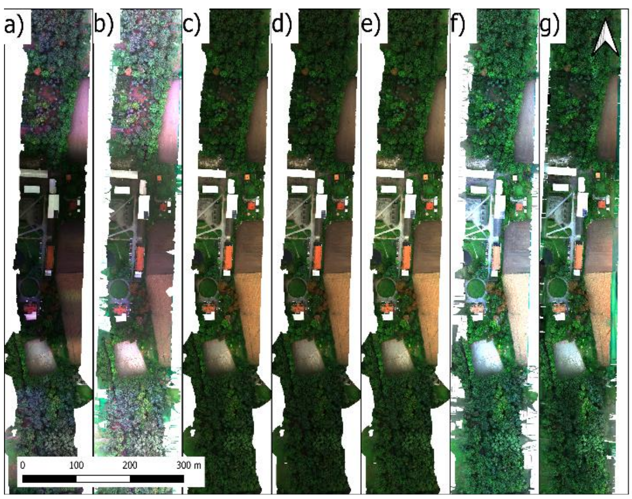

Figure 5. MSI variants of radiometric calibration in Gołuchów dataset: a) Metashape - without correction, b) ODM - without correction, c) Metashape – panel, d) Metashape - panel + sun sensor, e) Metashape - sun sensor, f) ODM – camera, g) ODM - camera + sun sensor

Table 1. Key characteristics of the datasets used for evaluating camera orientation and self-calibration in ODM and Metashape

No. of scenario	**1a**	**1b**	**2a**	**2b**	**3**
Dataset name	JOZE	Herby			Gołuchów
Image type	RGB				MSI
	nadir	oblique	nadir	oblique	nadir
UAV platform	DJI Mavic 3 Multispectral	DJI Phantom 4 RTK			DJI Matrice 300 RTK
Camera model	DJI M3M	DJI FC6310R			Micasense RedEdge-MX Dual
GCPs and ChPs	-		57 ChPs, 7 ChPs	29 ChPs, 5 GCPs	-
Focal length [mm]	12.29	8.8			5.5
Pixel size [µm]	3.36	2.41			3.75
Image resolution	5280 x 3956	5472 x 3648			1280 x 960
Field of view [°]	84	84			47.2
Image overlap [%]	85/75	90/90	90/90	90/90	80/80
Survey area [km^2]	0.024	0.071	0.117	0.071	0.268
Number of strips	12	16	7	16	3
Flying altitude [m]	87	46	56	46	85
GSD [cm]	2.2	1.2	1.5	1.2	6.3
Number of images	266	1102	1358	1102	500
Gimbal pitch angle [°]	0	45	0	45	0

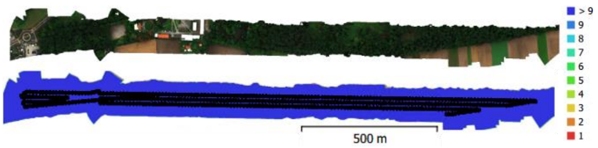

Figure 6. Overview of the nadir MSI (channels R: 6, G: 4, B: 2) dataset acquired in Gołuchów (scenario 3)

4. Methods

Several research scenarios were set up as part of the experiments conducted. Scenario 1a tested the orientation quality and camera calibration without the use of GCPs at different levels of the image pyramid for RGB nadir photos, while scenario 1b performed these tests for oblique images. Scenarios 2a and 2b investigated orientation accuracy and camera calibration quality at the original image resolution with the use of GCPs for RGB nadir and oblique images, while scenarios 3 concern the overview processing of MSI images and their calibration and orientation. All scenarios were also carried out in both ODM and Metashape, to compare the performance of the two software. A comparison of the operation of the two software programmes, ODM and Metashape, was limited to an analysis of calibration accuracy and data orientation.

Camera calibration was performed using different levels of the image pyramid. The comparison was made of how the individual parameters and values of the camera's interior orientation (focal length, Cx, Cy) and distortion coefficients (P1, P2, K1, K2, K3) change. All comparisons used the full set of Brown's model parameters. Plots of polynomials of the calculated calibrations were also generated radial and tangential distortions are computed based on the camera model parameters and visualized as a function of the pixel's distance from the image center. This allows for a clear comparison of geometric distortion magnitude across different calibration settings. The distortions are calculated using the following formulas:

$$dx = dx_{radial} + dx_{tangential} \qquad magnitude = \sqrt{dx^2 + dy^2}$$
$$dy = dy_{radial} + dy_{tangential}$$

The following study allowed the performance of the two programmes to be compared independently for nadir and oblique images. In addition, for the Herby (nadir and oblique) datasets for which measured points were available, the influence of the GCPs on the results of sensor orientation and calibration was investigated in both programs in the scenario with GCPs. In pre-processing, we used the same GCPs observations (number of points and measured image coordinates) in both programs.

ODM does not support using other types of measurement points besides GCPs (e.g., ChPs). The absence of ChPs makes it difficult to qualitatively compare orientation results with those from Metashape. However, in 2021, the developers announced plans to introduce functionality for manual Tie Points or ChPs (ODM, 2021). To enable a qualitative assessment of image calibration and orientation using GCPs (scenario 2a and 2b), the same ChPs as those measured in Metashape were manually identified localization on the orthomosaic and dense point cloud generated in ODM. The resulting RMS errors for these ChPs are presented and compared.

Due to lack of field spectral measurements for that area, only a qualitative assessment of radiometric quality of multispectral orthomosaic was possible to compare Metashape and ODM. For each software, all possible radiometric calibration processing scenarios were carried out (including variants without radiometric calibration). Then, a visual evaluation was performed to determine radiometric consistency within dataset depending on used method. Finally for each variant, histograms of every band were studied to evaluate reliability of reflectance values.

Processing was done using computer with Intel i9-12900KF 3.20 GHz processor, 128 GB of RAM and a 12 GB NVIDIA GeForce RTX 3080Ti GPU.

5. Results

The datasets presented in Table 1 were processed in ODM and Metashape software. For scenarios 1a and 1b no GCPs were used in the data alignment. However, different settings for image pyramid levels were used. The results of camera orientation in scenario 1a present in Tabel 2 (ODM) and Table 3 (Metashape).

As the processing pyramid level increases, the average reprojection error decreases from 2.03 to 1.13 in ODM and from 7.12 to 0.95 pix in Metashape. In both software, an error of approximately 1 pixel between the predicted and actual image locations indicates good quality of automatic point matching. The focal length stabilizes at 12.4842 mm in ODM and at 13.2718 mm in Metashape, which represents a considerable difference and may lead to significant discrepancies, particularly in depth estimation and the Z-coordinate of ground points in e.g., dense point cloud.

Table 2. The results obtained for processing scenario 1a, the JOZE dataset in the ODM software.

Level	Lowest	Low	Medium	High	Ultra
RMS GPS error [m]	0.003	0.011	0.033	0.052	0.055
Avg. Rep. Error [pix]	2.03	1.78	1.37	1.12	1.13
Focal [mm]	11.6947	11.8934	12.3245	12.4860	12.4842
Cx [µm]	8.87	7.10	7.10	8.87	8.70
Cy [µm]	-90.39	-89.06	-83.74	-81.08	-79.75
P1	-0.0001	-0.0001	-0.0001	-0.0004	-0.0004
P2	-0.0005	-0.0005	-0.0004	-0.0001	-0.0001
K1	-0.0818	-0.0928	-0.1053	-0.1094	-0.1093
K2	-0.0243	-0.0120	0.0022	0.0061	0.0062
K3	0.0028	-0.0029	-0.0167	-0.0213	-0.0216

Table 3. The results obtained for processing scenario 1a, the JOZE dataset in the Metashape software.

Level	Lowest	Low	Medium	High	Highest
RMS GPS error [m]	0.218	0.122	0.150	0.112	0.076
Avg. Rep. Error [pix]	7.12	3.32	1.50	1.17	0.95
Focal [mm]	13.7726	13.0379	13.4805	13.3928	13.2718
Cx [µm]	5.36	12.92	13.06	13.63	12.10
Cy [µm]	-77.33	-102.75	-90.32	-87.96	-90.68
P1	-0.0004	-0.0004	-0.0004	-0.0004	-0.0004
P2	-0.0004	-0.0002	-0.0002	-0.0003	-0.0003
K1	-0.1303	-0.1194	-0.1292	-0.1272	-0.1250
K2	-0.0024	-0.0087	0.0158	0.0129	0.0119
K3	-0.0240	-0.0288	-0.0410	-0.0367	-0.0343

The principal point coordinates show similar displacement trends in both programs; however, their estimated positions differ by approximately 1 pixel (1 pix it's 3.6 µm for the Mavic camera) for Cx and about 4 pixels for Cy. The distortion values are of the same order of magnitude in both cases.

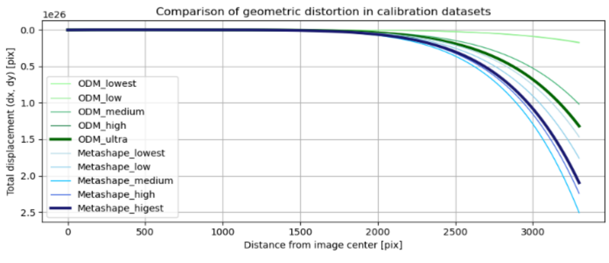

Figure 7. Comparison of calibration distortion polynomials for the JOZE dataset (scenario 1a) in two other software

To better visualize the discrepancies and compare the geometric distortion in the calibration datasets from Tables 2 and 3, calibration function plots are presented in Figure 7. It can be observed that at lower pyramid levels, both programs underestimate the calibration results (in opposite directions), but as the processing level increases, the functions converge. Ultimately, the difference in the estimated distortion at the corner of the frame camera image is approximately 0.7 pixels.

The results of camera orientation in scenario 1b (Herby oblique dataset) present in Table 4 (ODM) and Table 5 (Metashape).

Table 4. The results obtained for processing scenario 1b, the Herby Oblique dataset in the ODM software.

Level	Lowest	Low	Medium	High	Ultra
RMS GPS error [m]	0.001	0.013	0.27	0.038	0.037
Avg. Rep. Error [pix]	2.12	1.81	1.41	1.15	1.16
Focal [mm]	8.9003	8.9108	8.9108	8.9095	8.9082
Cx [µm]	-13.2	-43.5	-54.1	-63.3	-64.6
Cy [µm]	12.3	5.3	6.2	6.2	7.9
P1	0.0000	-0.0003	-0.0001	-0.0001	-0.0001
P2	-0.0003	-0.0011	-0.0013	-0.0013	-0.0013
K1	-0.0122	-0.0134	-0.0142	-0.0136	-0.0134
K2	0.0003	0.0003	0.0014	0.0001	-0.0005
K3	0.0051	0.0082	0.0079	0.0088	0.0094

Table 5. The results obtained for processing, the Herby Oblique dataset (1b scenario) in the Metashape software.

Level	Lowest	Low	Medium	High	Highest
RMS GPS error [m]	0.002	0.006	0.008	0.010	0.011
Avg. Rep. Error [pix]	5.66	2.52	1.54	0.97	0.77
Focal [mm]	8.8923	8.8963	8.9003	8.9011	8.8992
Cx [µm]	-47.60	-44.12	-44.95	-44.77	-45.19
Cy [µm]	29.35	27.30	23.57	21.80	22.35
P1	-0.0015	-0.0015	-0.0015	-0.0015	-0.0015
P2	-0.0002	-0.0001	-0.0001	-0.0001	-0.0001
K1	-0.0128	-0.0142	-0.0132	-0.0129	-0.0119
K2	-0.0020	0.0014	-0.0008	-0.0013	-0.0045
K3	0.0107	0.0080	0.0098	0.0099	0.0126

In the oblique image dataset, the Avg. Rep. Error is again notably lower for the original image resolution in Metashape (0.77 pix) compared to ODM (1.16 pix). In this case, the differences in the estimated focal length are no longer substantial, with values of 8.9082 mm in ODM and 8.8992 mm in Metashape. This is likely due to the fact that estimating the focal length from an oblique image dataset is generally more robust than from nadir-only imagery, where the differences were more pronounced. Oblique photographs offer improved geometric diversity and capture objects from multiple angles, which facilitates a more accurate focal length estimation.

Once again, relatively large differences in the estimated values of Cx and Cy are observed. It should be noted that Scenario 1b (Phantom 4) was performed using a different UAV platform than Scenario 1a. Calibration function plots for this dataset are presented in Figure 8. The estimated distortion difference between the Ultra level in ODM and the Highest level in Metashape is approximately 0.2 pixels.

In next step, we process the data according to scenarios 2a and 2b, and using the highest level of the image pyramid with GCPs. The results of camera self-calibration are presented in Table 6 and Table 7.

The Avg. Rep. Error for both nadir and oblique datasets with GCPs is noticeably lower in Metashape (from 1.19 to 0.61 pix and from 1.18 to 0.77 pix) compared to ODM. Once again, the discrepancy in the calibrated focal length is significantly higher in the nadir dataset than in the oblique one, which reflects the inherent differences in their image geometry, as previously discussed.

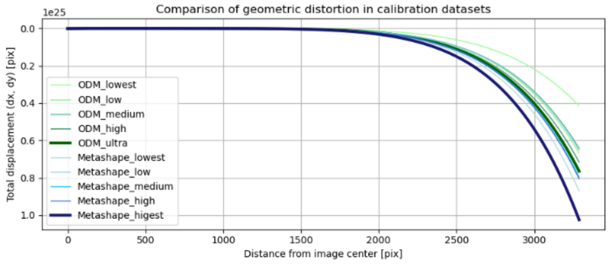

Figure 8. Comparison of calibration distortion polynomials for the Herby Oblique (scenario 1b)

Table 6. The results obtained for processing scenario 2a the Herby Nadir dataset with GCPs

Software & Settings	ODM (ultra)	Metashape (highest)
RMS GCPs X [m]	0.001	0.025
RMS GCPs Y [m]	0.000	0.026
RMS GCPs Z [m]	0.001	0.018
Total RMS GCPs [m]	0.001	0.040
Avg. Rep. Error [pix]	1.19	0.61
Focal [mm]	9.1970	8.9134
Cx [μm]	5.28	-39.46
Cy [μm]	38.68	23.17
P1	-0.0001	-0.0015
P2	-0.0016	-0.0001
K1	-0.0143	-0.0157
K2	-0.0001	-0.0016
K3	0.0104	0.0099

Table 7. The results obtained for processing scenario 2b the Herby Oblique dataset with GCPs

Software& Settings	ODM (ultra)	Metashape (highest)
RMS GCPs X [m]	0.002	0.015
RMS GCPs Y [m]	0.010	0.009
RMS GCPs Z [m]	0.004	0.023
Total RMS GCPs [m]	0.006	0.029
Avg. Rep. Error [pix]	1.18	0.77
Focal [mm]	8.9121	8.8998
Cx [μm]	-54.07	-45.02
Cy [μm]	7.03	23.85
P1	-0.0001	-0.0015
P2	-0.0013	-0.0001
K1	-0.0134	-0.0118
K2	-0.0007	-0.0045
K3	0.0098	0.0126

The estimated position of the principal point (Cx, Cy) in both datasets deviates much more than in scenarios 1a and 1b. This may be attributed to the Bundle Adjustment process and the weights assigned to different types of observations. For the GCPs, an accuracy of 3 cm for X/Y and 5 cm for Z was applied, corresponding to the expected precision of GNSS RTK measurements. For onboard camera positions (EOZ), an accuracy of 10 cm was set. Metashape allows for further refinement by assigning manual Tie Point measurement accuracy (0.5 pixels) and automated Tie Point accuracy (1 pix). ODM, however, does not provide options for specifying observation accuracy for either manual or automatic Tie Points. This lack of flexibility may partially explain the larger discrepancies in the estimated principal point positions shown in Tab 6 and 7. Moreover, the very low RMS error on GCPs observed in ODM – 0.1 cm (lower that RMS error in Metashape – 4 cm) suggests that these observations are weighted too strongly, possibly leading the adjustment to overfit their positions. As a result, this may distort the estimated interior parameters, particularly the principal point coordinates Cx and Cy.

Figure 8 presents the total distortion curves (radial and tangential combined) for both nadir and oblique datasets, as estimated by both softwares. The overall distortion appears to be well estimated, with differences between Metashape and ODM remaining below approximately 0.1 pixels for the nadir dataset and around 0.2 pixels for the oblique dataset.

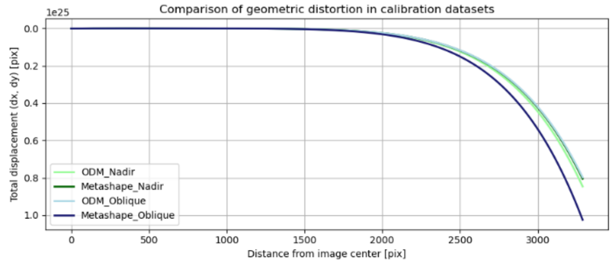

Figure 9. Comparison of calibration distortion polynomials for processing with GCPs the Herby Oblique and Herby Nadir (scenario 2a and 2b)

Table 8. The results obtained for processing scenario 2a and 2b (Herby Nadir and Oblique datasets with ChPs) In Metashape

	RMS Check Points [m]			
	X	Y	Z	Total
ODM Nadir	0.032	0.044	0.038	0.067
Metashape Nadir	0.022	0.016	0.026	0.038
ODM Oblique	0.045	0.063	0.036	0.085
Metashape Oblique	0.018	0.010	0.026	0.033

To evaluate the quality of image orientation and camera self-calibration, additional results based on ChPs were analyzed. In Metashape, these were conventional observations marked manually on images but excluded from the bundle adjustment. In contrast, due to the lack of native ChP support in ODM, the coordinates of ground markers were measured on the orthomosaic (XY) and point cloud (Z) using QGIS. The results are presented in Table 8. The RMS error on ChPs in ODM is approximately twice as high as in Metashape, (6.7 vs. 3.8 cm and 8.5 vs. 3.3 cm, respectively), suggesting that the accuracy of the generated outputs and the reliability of the orientation process in ODM require further investigation and validation in future studies.

The final step was to process the multispectral data according to scenarios 3. A dataset of 500 10-band images was processed in both softwares. In terms of multispectral data processing, ODM provides band alignment functionality required for multi-lens multispectral sensors but allows only a limited options of radiometric calibration methods. The method adopted in practice using calibration panels (with optional use of sun sensor depending on lighting conditions) is an integral part of the radiometric calibration process of images in Metashape. The DN values of the raw images in the 16-bit range are converted to reflectance values. For practical reasons, the output reflectance rasters are not floating point in the 0-1 range, but the range is stretched in half of the integer 16-bit space (range of 0-32768, where 32768 corresponds to reflectance equal to 1). ODM is limited only to correcting for sensor-related factors such as black-level, vignetting and allows the use of sun sensor metadata, which is a method that is not universal and does not provide sufficiently consistent results that enable, for example, multi-temporal analysis. Floating point values of the output reflectance rasters produced by ODM are within ranges of (-0.22; 0.20) and (-0.0004; 0.006) for “camera” and “camera+sun” radiometric calibration options respectively. Contrary to Metashape reflectance value distribution in NIR band, ODM results range is far from expected for such dataset (Fig. 10.). These values, despite decent visual output on the orthomosaic are questionable in terms of carrying absolute reflectance information.

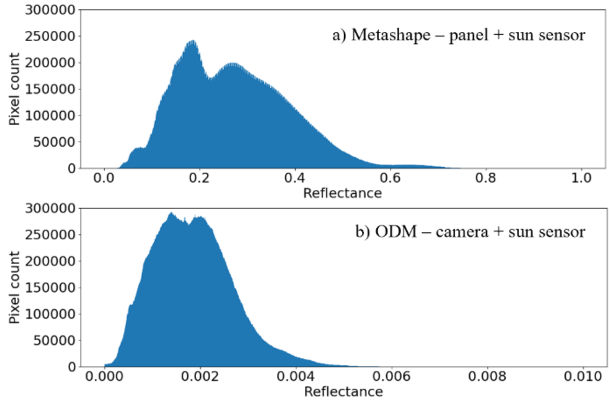

Figure 10. Reflectance value distribution in NIR band in variants using sun sensor metadata. a) Metashape, b) ODM. Variation in the reflectance ranges should be noted when comparing both figures.

6. Discussion and Conclusion

This study presents and compares four measurement scenarios aimed at evaluating the performance of two photogrammetric processing solutions: the open-surce ODM and the commercial Metashape. Additionally, a sample dataset processed from MSI images is discussed. Cameras installed in UAV cannot be considered as metric and stable imaging systems, therefore, simultaneous camera self-calibration is essential to obtain reliable results. This necessity is thoroughly examined is the presented scenarios. The measurement scenarios investigated include: 1a) RGB nadir images acquired with DJI Mavic 3, processed at different image pyramid levels, 1b) RGB oblique images acquired wih DJI Phantom 4 RTK, also processed at different image pyramid levels, 2a) Nadir RGB images form DJI Phantom 4 RTK with GCPs, used to analyze how onboard georeferencing affects image orientation and camera calibration, 2b) Oblique RGB images from the same platform, processed also with GCPs, to assess the impact of RTK-based georeferencing on calibration and orientation, 3) Processing of MSI images.

Scenarios 1a and 1b focused on evaluating the process of camera self-calibration and image orientation for both nadir and oblique UAV imagery, using the two software packages and various levels of image downsampling (image pyramid). The comparison included the interior camera orientation parameters — focal length, principal point coordinates (Cx, Cy) — and distortion coefficients (P1, P2, K1, K2, K3), applying the full Brown’s distortion model in all analyses.

In scenarios 2a and 2b, full-resolution nadir and oblique images were processed using GCPs. It is important to note that ODM currently lacks functionality for introducing ChPs or manuall Tie Points, which is a significant limitation in a photogrammetric context, as it restricts control over the quality and accuracy assessment of the outputs.

The conducted experiments demonstrated that the open-source solution can achieve comparable calibration results to Metashape. This is likely because both tools are based on the SfM approach for image orientation.

Results of self-calibration with and without GCPs did not differ significantly, suggesting that UAV flights equipped with RTK GNSS systems may provide sufficient georeferencing accuracy for many applications, even with minimal or no GCPs. This finding aligns with observations reported by, e.g., Przybilla et al. (2020). RTK-enabled UAV systems may be especially valuable in areas where GCPs measurement is difficult or impossible.

Moreover, in oblique flight missions, the camera calibration results between the two programs were more consistent. This can be attributed to improved scene geometry and greater depth variation in oblique imagery, which enhances the ability to model lens distortions more robustly.

Both Metashape and ODM handle the band alignment process well during multispectral imagery processing with no visible geometric misalignment between bands. Radiometric calibration of multispectral data in ODM is limited, does not support calibration panels and generates questionable reflectance values. While it does not completely disqualify ODM use in remote sensing approaches based on normalized indices, its reflectance values may not be reliable for multi-temporal analysis without calibration panels.

Acknowledgments

Multispectral dataset “Gołuchów” was acquired during final campaign of “Improving methods of acquisition and processing of remote sensing data from unmanned aerial vehicles” project carried out by Dragonfly Vision and Faculty of Geodesy and Cartography of Warsaw University of Technology.

Datasets Herby Nadir and Oblique were acquired for the project “R&D works in inventory and modelling of key technical and transport infrastructure objects in BIM technology using AI tools in the process of drone data processing”, financed by the National Centre for Research and Development, grant no POIR.01.01.01-00-0980/20. The project is being carried out by an interdisciplinary research team by SkySnap Sp. z o.o. Company and Faculty of Geodesy and Cartography of Warsaw University of Technology.

References

Agisoft LLC. (2025). Agisoft Metashape user manual: Professional Edition (Version 2.2). Agisoft LLC.

Burdziakowski, P. (2017). Evaluation of open drone map toolkit for geodetic grade aerial drone mapping – case study. International Multidisciplinary Scientific GeoConference Surveying Geology and Mining Ecology Management, SGEM, 17(23), 101-110.

DJI, 2025a: Phantom 4 RTK Technical Data, https://www.dji.com/de/phantom-4-rtk/info. Access:14.05.2025

DJI, 2025b: Phantom 4 RTK Technical Data, https://dji.com/pl/support/product/matrice-300. Access:14.05.2025

DJI, 2025c: Phantom 4 RTK Technical Data, https://ag.dji.com/mavic-3-m/specs. Access: 14.05.2025

Fryskowska-Skibniewska, A., Kedzierski, M., Sekrecka, A., Braula, A., (2016). Calibration of low cost RGB and NIR UAV cameras. *ISPRS - International Archives of the Photogrammetry, Remote Sensing and Spatial Information Sciences. XLI-B1. 817-821.*

Garcia, Y., de Oliveira, H. C., Fernandes, R., Costa, D., (2020). Evaluation of Different Methods for Non-Metric Camera Calibration. *Anuario do Instituto de Geociencias. 43. 266-272*.

Gbagir, A. M. G., Ek, K., & Colpaert, A. (2023). OpenDroneMap: multi-platform performance analysis. *Geographies*, *3*(3), 446-458.

Groos, A. R., Bertschinger, T. J., Kummer, C. M., Erlwein, S., Munz, L., & Philipp, A. (2019). The potential of low-cost UAVs and open-source photogrammetry software for high-resolution monitoring of Alpine glaciers: a case study from the Kanderfirn (Swiss Alps). *Geosciences*, *9*(8), 356.

Jełowicki, Ł., Sosnowicz, K., Ostrowski, W., Osińska-Skotak, K., & Bakuła, K. (2020). Evaluation of rapeseed winter crop damage using UAV-based multispectral imagery. *Remote Sensing*, *12*(16), 2618.

Kaimaris, D., Patias, P., & Sifnaiou, M. (2017). UAV and the comparison of image processing software. International Journal of Intelligent Unmanned Systems, 5(1), 18-27.

Kloc, B., Mazur, A., & Szumiło, M. (2021). Comparison of free and commercial software in the processing of data obtained from non-metric cameras. *Journal of Ecological Engineering, 22(2)*.

Martinez Batlle, J. (2018). Digital photogrammetry of historical aerial photographs using open-source software. *EarthArXiv eprints*, BNA95.

Mora-Félix, Z. D., Rangel-Peraza, J., Monjardin, S. & Sanhouse-García, A. (2024). Performance and precision analysis of 3D surface modeling through UAVs: validation and comparison of different photogrammetric data processing software. *Physica Scripta. 99.*

Näsi, R., Honkavaara, E., Blomqvist, M., Lyytikäinen-Saarenmaa, P., Hakala, T., Viljanen, N., ... & Holopainen, M. (2018). Remote sensing of bark beetle damage in urban forests at individual tree level using a novel hyperspectral camera from UAV and aircraft. *Urban Forestry & Urban Greening*, *30*, 72-83.

Nikolakopoulos, K. & Koukouvelas, J. (2017). Commercial vs professional UAVs for mapping. *Fifth International Conference on Remote Sensing and Geoinformation of the Environment, 1044409* (6 September 2017),

ODM. (2021). Feature Request: Additional Control Point Types #1302. https://github.com/OpenDroneMap/ODM/issues/1302

OpenDroneMap Authors. (2020). ODM - A command line toolkit to generate maps, point clouds, 3D models and DEMs from drone, balloon or kite images. OpenDroneMap/ODM GitHub Page. https://github.com/OpenDroneMap/ODM

OpenDroneMap GitHub repository, (2022) https://github.com/OpenDroneMap/ODM/blob/master/opendm/multispectral.py

Ostrowski, W. & Bakuła, K., (2016). Towards efficiency of oblique images orientation. *ISPRS - International Archives of the Photogrammetry, Remote Sensing and Spatial Information Sciences.* XL-3/W4. 91-96.

Ostrowski, W., Miszk, Ł., Modrzewski, J., Wilk, Ł., & Lech, P. (2024). Monitoring of large-scale archaeological excavations using photogrammetric techniques-Nea Paphos case study. *Journal of Archaeological Science: Reports*, *53*, 104353.

Patel, S., Chintanadilok, J., Hall-Scharf, B., Zhuang, Y., Strickland, J., & Singh, A. (2024). WebODM: An Open-Source Alternative to Commercial Image Stitching Software for Uncrewed Aerial Systems: AE593, 2/2024. *EDIS*, *2024*(1).

Pell, T., Li, J. Y., & Joyce, K. E. (2022). Demystifying the differences between structure-from-Motion Software packages for pre-processing drone data. *Drones*, *6*(1), 24.

Przybilla, H. J., Bäumker, M., Luhmann, T., Hastedt, H., & Eilers, M. (2020). Interaction between direct georeferencing, control point configuration and camera self-calibration for RTK-based UAV photogrammetry. The International Archives of the Photogrammetry, Remote Sensing and Spatial Information Sciences, 43, 485-492.

Rupnik, E., Nex, F. & Remondino, F., (2013). Automatic orientation of large blocks of oblique images. *ISPRS - International Archives of the Photogrammetry, Remote Sensing and Spatial Information Sciences.*

Shen, S. "Accurate Multiple View 3D Reconstruction Using Patch-Based Stereo for Large-Scale Scenes." IEEE Transactions on Image Processing 22, no. 5 (May 2013): 1901–14.

da Silva, T.v.d.W.; Gomes Pereira, L.; Oliveira, B.R.F. Assessing Geometric and Radiometric Accuracy of DJI P4 MS Imagery Processed with Agisoft Metashape for Shrubland Mapping. Remote Sens. 2024, 16, 4633.

Silva, L. Dias, F., Assis, V. C., Pinto, C. & Rangel, F. (2022). Validation of the positional accuracy of products resulting from the digital processing of UAV images. Brazilian Journal of Agricultural and Environmental Engineering, v. 26, n. 8, 624-630.

Triggs, B., McLauchlan, P. F., Hartley, R. I., & Fitzgibbon, A. W. (1999, September). Bundle adjustment—a modern synthesis. In *International workshop on vision algorithms* (pp. 298-372). Berlin, Heidelberg: Springer Berlin Heidelberg.

Vacca, G. (2020). WEB open drone map (WebODM) a software open source to photogrammetry process. In Fig Working Week 2020. Smart surveyors for land and water management.

Vivar-Vivar, E.D.; Pompa-García, M.; Martínez-Rivas, J.A.; Mora-Tembre, L.A. UAV-based Characterization of Tree-Attributes and Multispectral Indices in an Uneven-Aged Mixed Conifer-Broadleaf Forest. Remote Sens. 2022, 14, 2775.

Vong, A.; Matos-Carvalho, J.P.; Toffanin, P.; Pedro, D.; Azevedo, F.; Moutinho, F.; Garcia, N.C.; Mora, A. How to Build a 2D and 3D Aerial Multispectral Map?—All Steps Deeply Explained. Remote Sens. 2021, 13, 3227.